Int. J. Electrochem. Sci., 15 **(2020)** 9864 – 9873, doi: 10.20964/2020.10.20

International Journal of
ELECTROCHEMICAL
SCIENCE
www.electrochemsci.org

Influence of Threshold Chloride Concentration on Corrosion Behavior of Low-Alloy Steel Rebar in Concrete Pore Solutions

Ziyi Zhang[*]

School of Civil and Construction Engineering, Oregon State University, Kearney Hall, 1491 SW Campus Way, Corvallis, OR 97331
[*]E-mail: zhangziyitg@sina.com

Received: 19 May 2020 / *Accepted:* 16 July 2020 / *Published:* 31 August 2020

Corrosion of steel reinforced concrete by the chloride-induced is the most common types of degradation in the building and construction industry. Here, the corrosion behavior of Chromium (Cr)-modified low-carbon and low-alloy steel rebars exposed to simulated concrete pore solution (SCPS) with different chloride content were studied by the electrochemical impedance spectroscopy (EIS) technique. EIS results indicate that Cr-modified low-alloy steel reveal a higher corrosion protection with a high level of threshold chloride in SCPS and higher impedance than the low-carbon steel. The double-layer capacitance values were reduced as pH value gradually increased, which indicates that the thickness of the passive layer was enhanced, resulting in an increase in the protective capacity. Scanning electron microscopy investigation confirmed the results attained by EIS measurement. The findings show that low-alloy steel indicates higher resistance of pitting corrosion because of the formation of Cr-enriched stable and protective rust layer.

Keywords: Threshold chloride level; Low-alloy steel rebar; Simulated concrete pore solution; Electrochemical impedance spectroscopy

1. INTRODUCTION

Premature degradation of reinforced concrete causing caused by immersion in aggressive environment is a serious challenge that contractors, designers and engineers are facing [1-3]. Marine environments and the widespread use of de-icing salts may cause the passive layer to rupture, allowing the surface of steel to act as coupled cathodic and anodic reaction cell that accompanies corrosion processes [4, 5]. Chloride-induced corrosion of reinforced concretes have been considered under different conditions in recent decades, typically about the value of chloride threshold (VCT) [6, 7]. VCT was introduced as the chloride content related to the depassivation of the rebar in non-carbonated alkaline concrete [8, 9] which only studied the early stage of corrosion. However, VCT states to chloride content, which causes visible damage in reinforced concrete structures [10, 11]. Much effort had been made to determine the VCT of reinforced concrete, but the values attained vary considerably.

This can be associated to many factors. The external environment is the first factor such as outdoor, with constant laboratory conditions, its relative humidity and variable temperature. The second factor is the test environment such as concrete, mortar or simulated pore solution [12-14]. The third and fourth cases are related to the surface condition of rebars and the measurement methods [15, 16]. The major factors in VCT have been recognized as the pH of the pores concrete solution, chemical composition of steel rebars, temperature and their electrochemical potential of steel [17-19].

However, it is commonly recognized that a good passive effect plays an important role in the corrosion protection of steel alloys in concrete [20, 21]. Little research so far has been done on the effect of passive layer on corrosion protection caused by chloride ions in low-alloy steel rebars. Therefore, in this study, the effect of chloride content, pH value of aggressive environment and exposure time on the corrosion behavior of low-carbon and low-alloy steel rebars into simulated concrete pore solution were considered using electrochemical impedance spectroscopy.

2. MATERIALS AND METHODS

In this study, steel rebars with 15 mm diameter and 25 cm long were used for investigation of corrosion behavior of steel bars in simulated concrete pore solution (SCPS) environment. The surfaces of all steels were easily cleaned using acetone solution, washed in DI water and left to dry by putting on air. Epoxy-coated steel was done in the ends of steel bars. Two types of steels, namely low-alloy and low-carbon steels, were investigated. The chemical composition of steel bars used in this study are shown in Table 1.

Table 1. Chemical compositions of steel bars

Steels	**Chemical compositions (wt%)**						
	Fe	C	Mn	Si	P	S	Cr
Low-carbon	Bal.	0.25	1.55	0.56	0.023	0.011	0.0
Low-alloy	Bal.	0.23	1.55	0.45	0.012	0.008	5.07

The SCPS was prepared using a mixture of 0.2 M NaOH, 0.5 M KOH and0.3 M $Ca(OH)_2$.The pH value of the solution was adjusted by adding various amount of sodium bicarbonate in 10.5, 11.5 and 12.5 and calibrating through pH meter. The electrochemical tests were performed by three-electrode electrochemical cell setup. A steel bar, a saturated calomel and a graphite electrodes as working electrode, reference and counter electrodes, respectively. The steel rebars were immersed into the SCPS with three concentrations of NaCl, 0.1M, 0.3M and 1.0M as low, close and high to threshold chloride content respectively, for assessment of pitting corrosion behavior [22]. For pre-passivation case, the steel rebars were exposed to chloride-free SCPS for one week for the formation of a stable passive layer before the addition of chlorides [23].

Electrochemical impedance spectroscopy (EIS) technique was done in the frequency range from 0.1 MHz to 0.1 mHz at the open circuit potential with ±10 mV AC perturbation. The morphologies of steel rebars were studied by a Zeiss Sigma scanning electron microscope (SEM).

3. RESULTS AND DISCUSSION

The Bode plots of the low carbon and low alloy steels are shown in Figure 1. Two time constants are detected for both the corrosion and the passivation stage. Figure 1indicates the modulus and phase angle plots for both steel rebars were unexpectedly reduced after one-week passivation in chloride-free SCPS environment. The passivation behaviors of steel rebars in the presence of chloride ions had changed considerably compared to those under chloride-free environment. Furthermore, the low-alloy steel showed more passivation behaviors than low-carbon steel which can be attributed to the surface properties of low-alloy steel with few defects and micro-cracks, assisting the formation of a protective and dense passive layer.

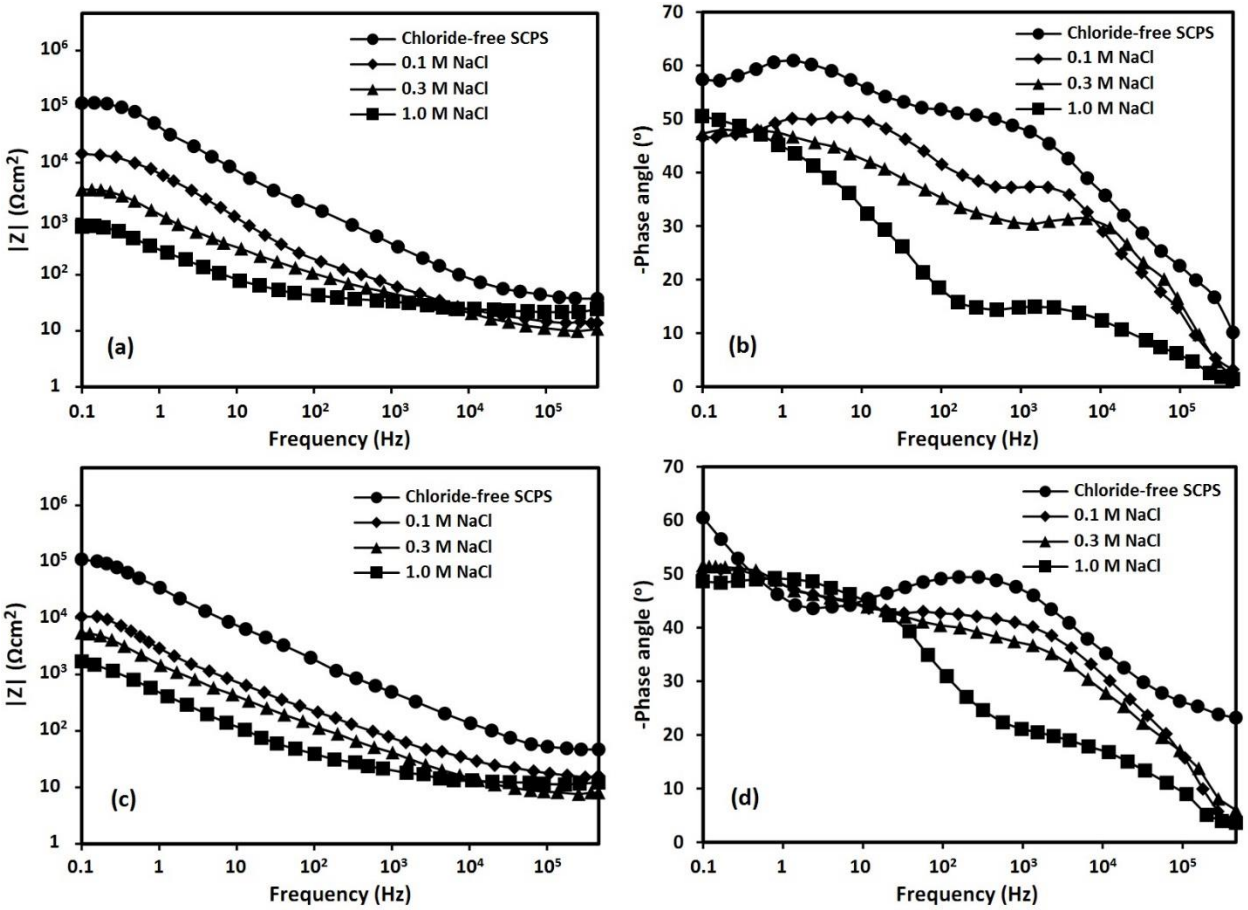

Figure 1. Bode plots of low-carbon and low-alloy steel in SCPS with various NaCl concentrations after one week exposure times

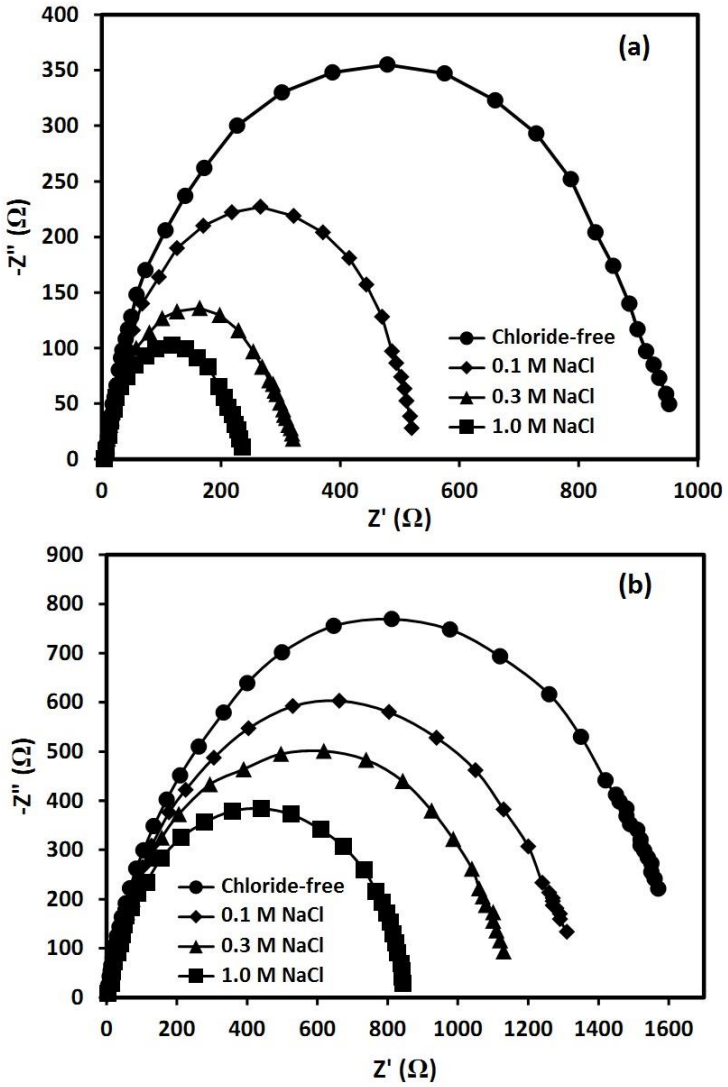

Figure 2. EIS plots of (a) low-carbon and (b) low-alloy steels exposed to SCPS with various NaCl concentrations after one week exposure times

EIS technique has been widely used in the investigation of the passive film because of its capability to evaluate redox reactions of steels in SCPS environment [24, 25]. The EIS plots of low-carbon and low-alloy steels exposed to SCPS with various NaCl concentrations after one-week exposure time are indicated in Fig. 2. Nyquist diagrams typically show a capacitive loop in both steels that its diameter decreased with increasing NaCl concentrations. It may be ascribed to corrosion behavior of Cl ions on the steel surface. Figure 3 shows an equivalent circuit model which proposed to simulate these electrochemical process of steel rebars. R_s is the SCPS resistance. At higher frequencies, R_f and C_f show a resistance because of the ionic paths by the oxide film and capacitive behavior of formed passive layer, respectively [26, 27]. At the second time constant, R_{ct} and C_{dl} reveals the charge-transfer resistance and the capacitive behavior in the interfaces [28]. The best fitting parameters based on the circuit depicted in figure 3 are summarized in Table 2.

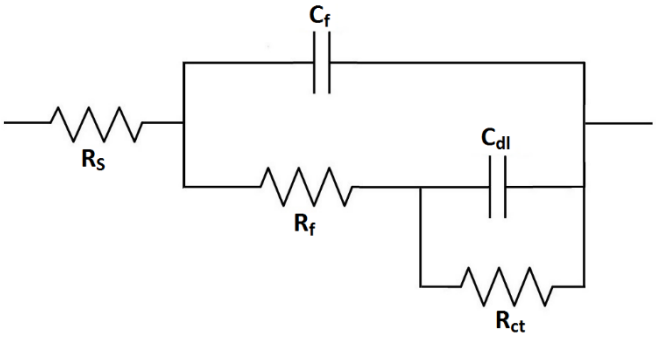

Figure 3. An equivalent circuit model

As revealed, the R_{ct} values considerably reduced from 982 Ω to 238 Ω and 1623 Ω to 846 Ω for low-carbon and low-alloy steels, respectively, by the addition of NaCl in the SCPS environment, indicating the chloride presence led to an increase in corrosion on the surface of steel.

Table 2. Electrochemical parameters achieved from the fitted equivalent circuit

Steel	**NaCl content in** SCPS	**R_s (Ω)**	**C_f (μFcm^{-2})**	**R_f (Ω)**	**C_{dl} (μFcm^{-2})**	**R_{ct} (Ω)**
Low-carbon	**Chloride free**	27	4.9	548	6.1	982
	0.1 M	25	8.2	282	9.7	532
	0.3 M	29	9.9	175	11.2	327
	1.0 M	23	11.3	124	12.4	238
Low-alloy	**Chloride free**	32	1.7	912	2.2	1623
	0.1 M	28	2.6	723	3.7	1374
	0.3 M	34	3.5	585	4.8	1172
	1.0 M	31	5.9	423	7.2	846

Moreover, table 2 shows that R_f gradually reduced by increasing the concentration of Cl ions which reveals that porous and nonprotective products have been developed on the surface of both steels. These findings are consistent with the best-fit results for C_{dl} which were gradually increased over 12.4 and 1.2 μFcm^{-2} with 1 M NaCl in SCPS for low-carbon and low-alloy steels respectively, indicating that produced corrosion can happen on the steel surface [29]. It can be related to the broken passive layer on the steel surface, when the Cl concentration was in the threshold value [30]. Furthermore, the low value of C_{dl} and the high value R_{ct} were found in low-alloy steel rebar compared to the low-carbon steel samples that can be attributed to the larger passive film thickness in low-alloy caused by the presence of Cr element.

EIS was done to characterize the effect of pH changes on the corrosion resistance of steels with passive films in the SCPS environment. As shown in Fig. 4, when pH value increased, the arc radius increased in both steel bars that reveals the enhancement of the corrosion behavior for steel bars.

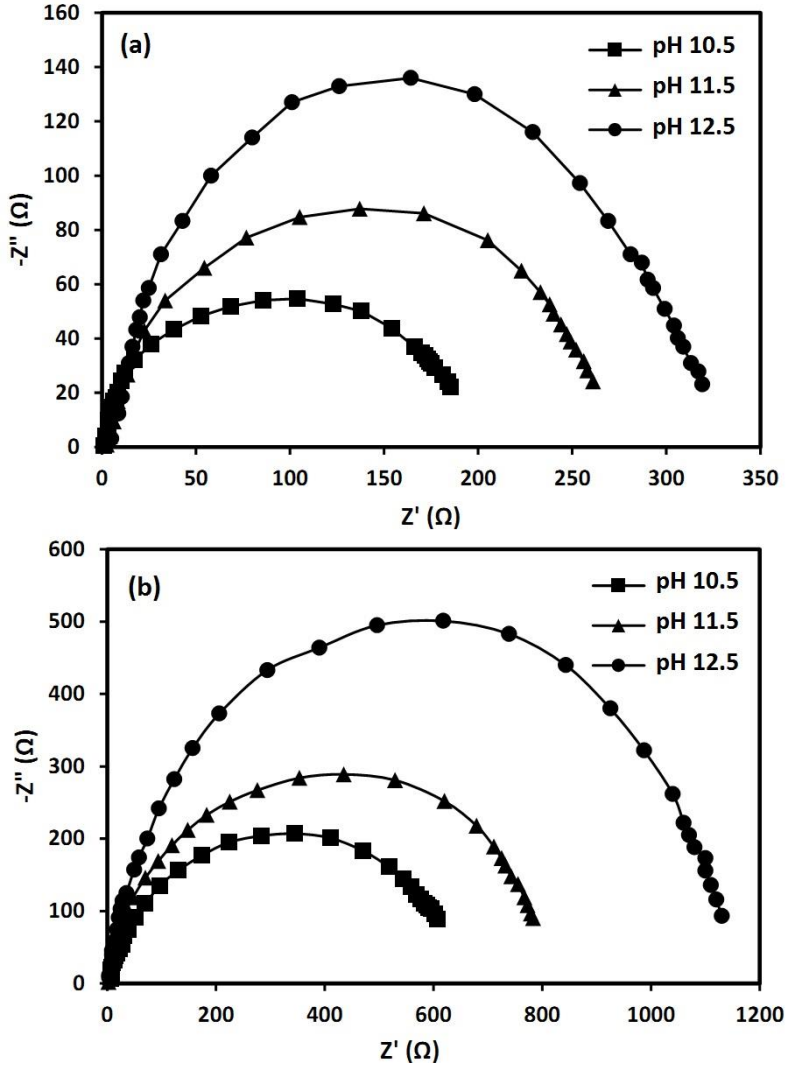

Figure 4. Nyquist plots of (a) low-carbon and (b) low-alloy steels in SCPS with various pH value after one week exposure times

Table 3. Electrochemical parameters achieved from the fitted equivalent circuit

Steel	pH	R_s (Ωcm^2)	C_f($\mu F cm^{-2}$)	R_f (Ωcm^2)	C_{dl} ($\mu F cm^{-2}$)	R_{ct} (Ωcm^2)
Low-carbon	10.5	26	11.7	102	13.9	198
	11.5	34	10.8	148	12.3	275
	12.5	29	9.9	175	11.2	327
Low-alloy	10.5	32	7.3	371	8.8	643
	11.5	25	5.2	467	6.5	821
	12.5	34	3.5	585	4.8	1172

The thickness of the passive layer can be measured with the following equation [31]:

$$D = \frac{\varepsilon \varepsilon_0 A}{C_{dl}} \quad (1)$$

Where D is the passive film thickness, ε_0 (8.85×10^{-12} F m^{-1}) and ε (12 for Fe oxides) are the vacuum permittivity and dielectric constant, respectively. A is an effective area and capacitance.

As indicated in table 3, the value of C_{dl} decreases as the pH value increases, which reveals that the passive film thickness was increased and the resulting protective capacity was enhanced when the pH value of solution was gradually increased.

Polarization resistance ($R_p = R_f + R_{ct}$) is recognized as a calculable indicator to investigate the corrosion resistance of steels in the aggressive environment [32]. Such that the higher value of R_p shows higher corrosion resistance value for the steel rebar. According to table 3, the low-alloy steel indicates higher value of R_p than the low-carbon steel at a constant pH value which can be associated to the creation of passive layer, showing a small amount of chromium micro-alloy into the steel assisted to form stable passive layers.

Moreover, increasing the pH values of SCPS showed a significantly development of R_p value exhibiting a higher corrosion protection for both steel rebars in pH 12.5.

Comparing C_f and C_{dl} in all samples (table 3), it is observed that C_f value is lower than C_{dl} indicating the formation of double layer and thin passive film at the interfaces have a high capacitive behavior.

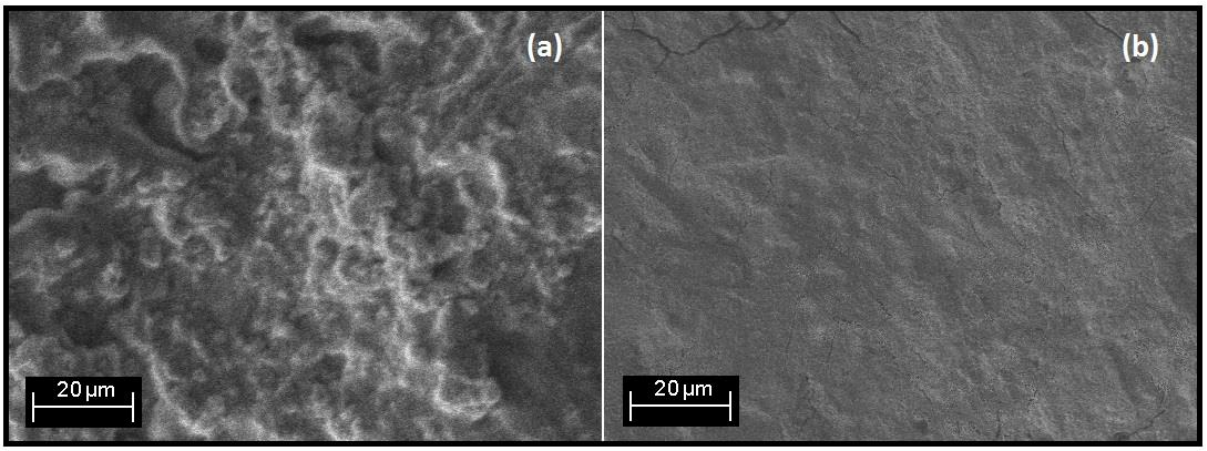

Figure 5. FESEM images of (a) low-carbon and (b) low-alloy steel rebars exposed to SCPS with 1 M NaCl after two weeks immersion times at pH 12.5.

Figure 5 indicates the FESEM morphology of low-carbon and low alloy steel rebars exposed to SCPS with 1 M NaCl after two weeks immersion times at pH 12.5. As shown in figure 5a, wide corrosion was detected on the surface of low-carbon steel, revealing the active corrosion state. Furthermore, very few small pits can be seen on the surface of low-alloy steel (Figure 5b), signifying that the low-alloy steel had an appropriate corrosion resistance in SCPS environment. These findings show that adding a small amount of chromium micro-alloy into the steel improves the corrosion behavior of steel rebars which is in accordance with the results obtained from electrochemical tests.

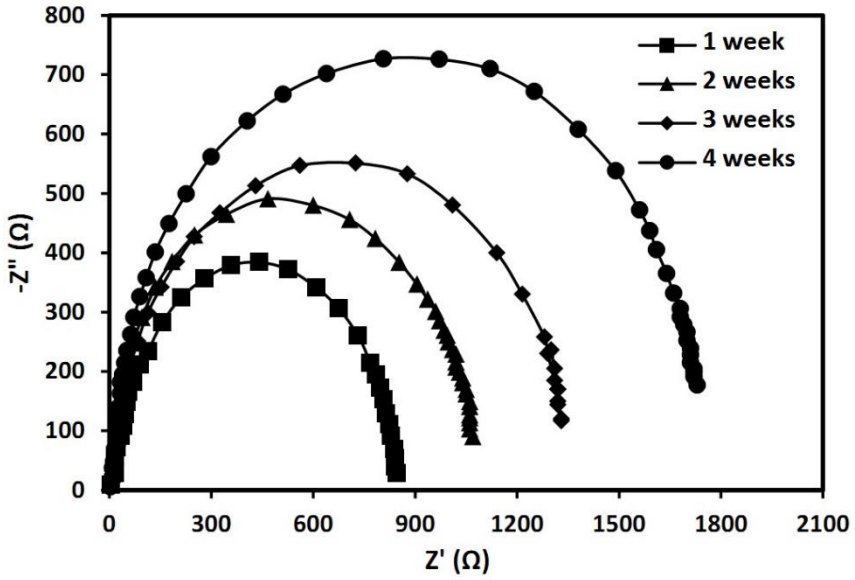

Figure 6. EIS plots of the low-alloy steel rebar exposed to SCPS with 1 M NaCl at different immersion times at pH 12.5.

Table 4. Electrochemical parameters achieved from the fitted equivalent circuit

Exposure time (week)	R_m (Ω)	R_f (Ω)	C_f (μFcm^{-2})	R_{ct} (Ω)	C_{dl} (μFcm^{-2})
1	31	423	5.4	846	7.2
2	27	458	5.1	1097	5.6
3	22	512	5.0	1353	3.5
4	26	534	5.2	1796	1.3

Figure 6 reveals Nyquist plots of low-alloy steel rebars exposed to SCPS with 1 M NaCl at different immersion time in pH 12.5. Table 4 indicates electrochemical parameters obtained from the fitted equivalent circuit. Results show that the R_{ct} was increased about two times from 1 to 4 weeks immersion time, with a decrease in the C_{dl} values from 7.2 to 1.3 μFcm^{-2}, probably because of higher density hydration products and pores of the steel rebar after four weeks immersion time. These results are in agreement with previous studies [33]. Furthermore, the C_f values were remained stable for all immersion time, indicating that no degradation in the protecting oxide-layer on the low-alloy steels, as expected for limited immersion time.

4. CONCLUSIONS

In this work, the corrosion behavior of Cr-modified low-alloy steel and low-carbon steel rebars exposed to SCPS with different chloride content were investigated by the EIS technique. Passive layer formed on the surface of steel rebar could increase chloride-induced corrosion resistance of low-carbon and low-alloy steels in SCPS with different chloride concentrations. When concentration of NaCl as chloride source in the SCPS increased to 1.0 M, low-alloy steel indicated superior corrosion resistance than low-carbon steel that can be attributed to a gradual formation of Cr-enriched rust layer into the

low-alloy steel, resulting in efficiently suppressing the diffusion of corrosion pits. The double-layer capacitance values were reduced as pH value gradually increased, which indicates that the thickness of passive layer enhanced, resulting protective capacity increased.

References

1. M.G. Sohail, R. Kahraman, N.G. Ozerkan, N.A. Alnuaimi, B. Gencturk, M. Dawood and A. Belarbi, *Journal of Performance of Constructed Facilities*, 32 (2018)
2. H. Karimi-Maleh and O.A. Arotiba, *Journal of colloid and interface science*, 560 (2020) 208.
3. S. Kakooei, H.M. Akil, M. Jamshidi and J. Rouhi, *Construction and Building Materials*, 27 (2012) 73.
4. L. Coelho and M.-G. Olivier, *Corrosion Science*, 136 (2018) 292.
5. F. Tahernejad-Javazmi, M. Shabani-Nooshabadi and H. Karimi-Maleh, *Composites Part B: Engineering*, 172 (2019) 666.
6. A. Kenny and A. Katz, *Construction and Building Materials*, 244 (2020) 118376.
7. C. Li, L. Jiang and S. Li, *Cement and Concrete Research*, 131 (2020) 106018.
8. J. Shi, J. Ming and W. Sun, *Corrosion Science*, 133 (2018) 288.
9. R. Dalvand, S. Mahmud and J. Rouhi, *Materials Letters*, 160 (2015)
10. X. Feng, R. Shi, L. Zhang, Y. Xu, X. Zhang, J. Zhang, Y. Ding, D. Chen, N. Ju and X. Zhang, *International Journal of Electrochemical Science*, 13 (2018) 2745.
11. H. Karimi-Maleh, K. Cellat, K. Arıkan, A. Savk, F. Karimi and F. Şen, *Materials Chemistry and Physics*, 250 (2020) 123042.
12. H. Shan, Z. Wang, J. Xu and L. Jiang, *International Journal of Electrochemical Science*, 13 (2018) 1120.
13. A. Khodadadi, E. Faghih-Mirzaei, H. Karimi-Maleh, A. Abbaspourrad, S. Agarwal and V.K. Gupta, *Sensors and actuators b: chemical*, 284 (2019) 568.
14. M. Miraki, H. Karimi-Maleh, M.A. Taher, S. Cheraghi, F. Karimi, S. Agarwal and V.K. Gupta, *Journal of Molecular Liquids*, 278 (2019) 672.
15. A. Fahim, P. Ghods, O.B. Isgor and M.D. Thomas, *Materials and Corrosion*, 69 (2018) 1784.
16. J. Rouhi, S. Mahmud, S. Hutagalung and S. Kakooei, *Micro & Nano Letters*, 7 (2012) 325.
17. R.B. Figueira, A. Sadovski, A.P. Melo and E.V. Pereira, *Construction and Building Materials*, 141 (2017) 183.
18. M. Liu, X. Cheng and X. Li, *International Journal of Electrochemical Science*, 14 (2019) 726.
19. H. Karimi-Maleh, F. Karimi, S. Malekmohammadi, N. Zakariae, R. Esmaeili, S. Rostamnia, M.L. Yola, N. Atar, S. Movagharnezhad and S. Rajendran, *Journal of Molecular Liquids*, (2020) 113185.
20. M. Dadfar, M. Salehi, M. Golozar, S. Trasatti and M. Casaletto, *International Journal of Hydrogen Energy*, 42 (2017) 25869.
21. Z. Ai, J. Jiang, W. Sun, D. Song, H. Ma, J. Zhang and D. Wang, *Applied Surface Science*, 389 (2016) 1126.
22. M. Ormellese, L. Lazzari, S. Goidanich, G. Fumagalli and A. Brenna, *Corrosion Science*, 51 (2009) 2959.
23. E. Volpi, A. Olietti, M. Stefanoni and S.P. Trasatti, *Journal of Electroanalytical Chemistry*, 736 (2015) 38.
24. H. Karimi-Maleh, M. Sheikhshoaie, I. Sheikhshoaie, M. Ranjbar, J. Alizadeh, N.W. Maxakato and A. Abbaspourrad, *New Journal of Chemistry*, 43 (2019) 2362.
25. J. Rouhi, S. Mahmud, S.D. Hutagalung and N. Naderi, *Electronics letters*, 48 (2012) 712.
26. H. Luo, H. Su, C. Dong and X. Li, *Applied Surface Science*, 400 (2017) 38.

27. N. Naderi, M. Hashim and J. Rouhi, *International Journal of Electrochemical Science*, 7 (2012) 8481.
28. S. Kakooei, H.M. Akil, A. Dolati and J. Rouhi, *Construction and Building Materials*, 35 (2012) 564.
29. K. Tang, *Corrosion Science*, 152 (2019) 153.
30. D. Sazou, M. Pavlidou and M. Pagitsas, *Journal of Electroanalytical Chemistry*, 675 (2012) 54.
31. V. Maurice, H. Peng, L.H. Klein, A. Seyeux, S. Zanna and P. Marcus, *Faraday discussions*, 180 (2015) 151.
32. H. Zhou, Y. Wang and T. Ma, *International Journal of Electrochemical Science*, 15 (2020) 3003.
33. M.O. Bragança, K.F. Portella, M.M. Bonato and C.E. Marino, *Construction and Building Materials*, 68 (2014) 650.